Antarct. Meteorite Res., 12, 1–18, 1999

PETROLOGICAL AND MINERALOGICAL STUDY OF ENSTATITE CHONDRITES WITH REFERENCE TO THEIR THERMAL HISTORIES

Makoto KIMURA[1] and Yangting LIN[2]

[1] *Institute of Astrophysics and Planetary Science, Faculty of Science, Ibaraki University, Mito 310-8512*
[2] *Guangzhou Institute of Geochemistry, Chinese Academy of Sciences, Guangzhou 510640, China*

Abstract: We investigated the complicated thermal histories of 8 Antarctic enstatite chondrites. In this report we present results of our mineralogical and petrological studies. Three of them (Yamato (Y)-791790, 791810 and 791811) are EH4 chondrites, but experienced higher temperature events in comparison with most of the other EH4s. Y-791790 includes a shock-induced melt vein. Y-86760 is recognized as a new EH melt rock that cooled rapidly from high temperatures. Absences of daubreelite in the EH4s and roedderite and forsterite in the melt rocks are consistent with such high temperature events. We infer that the parent body (or bodies) of EH chondrites experienced heavy impacts after or during metamorphism. Some EH4s and melt rocks cooled rapidly from high temperatures near the surface of the parent body, whereas the others cooled slowly in the depth of the parent body or were later reheated. Y-791510 contains glassy matrix unusually enriched in CaO, in the interstices among enstatite grains. The opaque mineralogy of Y-791510 is inconsistent with that of EH or EL. We propose that Y-791510 represents a new grouplet of enstatite chondrites.

1. Introduction

Enstatite (E) chondrites are the most reduced chondrites. Like ordinary chondrites, they are classified into petrologic types 3 to 6 (or 7). However, ZHANG *et al.* (1995) showed that the petrologic types of enstatite chondrites are not always consistent with the geothermometry or mineral chemistry, and suggested that the mineral chemistry is related to the conditions during brecciation after metamorphism to have determined petrologic types. On the other hand, some melt rocks or melt breccias have recently been discovered in E chondrites (*e.g.*, MCCOY *et al.*, 1995; RUBIN *et al.*, 1997; WEISBERG *et al.*, 1997). LIN and KIMURA (1998) also noticed that four Antarctic EH chondrites are melt rocks. Three of them (Yamato (Y)-8404, Y-8414 and Y-86004) cooled rapidly after complete melting perhaps near the surface of the parent body, whereas a melt rock, Y-82189, shows low-temperature equilibration. In Y-82189, we reported the first finding of F-phlogopite in enstatite meteorites. LIN and KIMURA also discovered that Y-793225 represents a new grouplet of E chondrites, which shows intermediate petrographical and mineral features between EH and EL groups. Thus, the thermal history and taxonomy of E chondrites may be much more diverse and complicated than considered before.

Here we report petrological and mineralogical features of 7 Antarctic E chondrites and Abee, following our previous work (LIN and KIMURA, 1998), in order to explore the thermal histories of E chondrites.

2. Samples and Analytical Procedure

We investigated 8 polished thin sections: Y-791790,51-2 (E3 after YANAI and KOJIMA, 1995), Abee,51-1 (EH4), Allan Hills (ALH)-77156,51-2 (EH4), Y-791810, 51-1 (E4), Y-791811,51-1 (E4), Y-86760,51-1 (E5), Y-791510,51-2 (E5) and Y-793258,51-1 (E6). For comparison, we also studied another set of thin sections, Y-791790,51-3, Y-791810,51-2, Y-791811,51-2, Y-86760,51-2 and Y-791510,51-1 under the optical microscope.

The thin sections were investigated with a JEOL 733 electron microprobe. The analytical procedure was the same as that outlined by LIN and KIMURA (1998). Modal compositions of the samples were also calculated by the same mode scanning procedure as given by LIN and KIMURA.

3. Petrography

All meteorites studied here mainly consist of enstatite with plagioclase, kamacite, troilite, (Mg,Mn,Fe) S. Table 1 gives the classification and modal compositions of these meteorites. Y-791510 and Y-791811 are heavily weathered. The shock degrees range from S2 to S3, according to the criteria by RUBIN *et al.* (1997).

ALH-77156: This chondrite shows the typical type 3 chondritic texture, including abundant chondrules often with glassy groundmass. Clinoenstatite, (50–300 μm) is more abundant than orthoenstatite. Some chondrules contain enstatite phenocrysts with forsterite inclusions. Roedderite occurs as isolated grains. Perryite, djerfisherite, phases A/B (not well characterized Cr-S phases) and niningerite are present. Phases A/B and niningerite are heavily weathered. We did not find oldhamite, probably because it was removed by weathering. Graphite occurs in two morphologies: spherulitic and laths in kamacite.

Y-791790, Y-791810 and Y-791811: These meteorites consist of chondrules, their fragments and isolated grains, with little chondritic matrix (Fig. 1a). Orthoenstatite as well as clinoenstatite (50–200 μm) are common. Forsterite often occurs within enstatite grains. Chondrule groundmasses are devitrified glasses. These chondrites contain niningerite and roedderite. From these findings, they are EH4 chondrites. The occurrences of forsterite and FeO-bearing pyroxene as mentioned below, also support this classification, based on the criteria by ZHANG *et al.* (1995). These meteorites could be paired according to their similar textures and modal abundances (Table 1). The noble gas data also support this suggestion (PATZER and SCHULTZ, 1998). Y-791790 contains a vein, mainly consisting of gray area with aggregates of dendritic metallic Fe-Ni and troilite (Fig. 1c). The gray area seems to be homogeneous and comprise silicate, mixed with abundant tiny opaque mineral spherules ($< 1\,\mu$m). It is not yet evident whether the silicate is glass or fine-grained aggregate. Based on the calculation from areas in back-scattered electron (BSE) images, the vein consists of 76 vol%

Table 1. Modal compositions of 8 enstatite chondrites (vol%).

Chondrite	ALH-77156	Y-791790	Y-791810	Y-791811	Abee	Y-86760	Y-791510	Y-793258
Classification	EH3	EH4	EH4	EH4	EH melt	EH melt	E anomalous	EL6
Shock stage	S3	S3	S2	S2	S3	S2	S3	S2
Forsterite	1.1	0.3	0.2	0.2				
Enstatite	69.5	68.0	63.8	58.6	57.3	50.6	68.1	62.9
Plagioclase*	5.0	7.8	7.1	9.8	12.8	17.8	4.5	15.8
Silica	1.1	3.3	1.5	3.9	1.7	7.5	0.2	0.1
Roedderite	0.4	0.8	1.2	0.1				
Metallic Fe-Ni	8.5	12.5	13.3	4.8	15.4	2.2	0.8	3.6
Schreibersite	1.0	1.5	1.5	1.1	0.3	0.3	0.3	0.9
Perryite	+							+
Graphite	+	+	+					+
Troilite	7.6	4.2	4.9	8.0	6.8	7.9	1.4	7.2
Daubreelite	0.5						0.2	0.6
(Mg,Mn,Fe)S	0.5	0.5	0.3	0.9	5.3	4.3		0.6
Oldhamite					0.1			
Sphalerite	+	+	+		+	+		
Djerfisherite	0.6							
Phases A/B	0.2							
Weathering	4.2	1.2	6.1	12.6	0.2	9.3	24.6	8.4

*: including glass in ALH77156 and Y-791500
+: trace

silicate, with 9% tiny opaque spherules, and 15% opaque mineral aggregates (8% metallic Fe-Ni and 7% troilite). In the host around the vein, silicate minerals do not show any evidence for melting and shock-induced deformation features such as mosaicism or maskelynite.

Y-86760: This meteorite has no chondrules, their relics or other clasts. Euhedral lathes of orthoenstatite (20–200μm) (Figs. 1d and e), are predominant, and are abundantly enclosed in metallic Fe-Ni and troilite. Anhedral plagioclase, silica mineral and opaque minerals fill the interstices among enstatite grains. Such textural features are typical of the other melt rocks (Y-8404, Y-8414 and Y-86004) (LIN and KIMURA, 1998). Relic grains, characterized by irregularly shaped, dusty features and so on, are often reported from impact-melted ordinary chondrites (*e.g.*, YAMAGUCHI *et al.*, 1998). However, such grains are not encountered in these EH melt rocks. The modal composition of Y-86760 (51 vol% enstatite, 8% silica mineral, 15% total opaque minerals, and 18% plagioclase) is within the range of Y-8404 and others (35–54% enstatite, 3–12% silica mineral, 15–31% total opaque, and 8–11% plagioclase). The higher plagioclase abundance in Y-86760 is an exception. Y-86760 seems to be paired with Y-8404 and others. All these melt rocks do not contain forsterite, roedderite, perryite, djerfisherite or phases A/B.

Abee: RUBIN and SCOTT (1997) argued that it is an EH melt breccia, mainly consisting of euhedral orthoenstatites grains. The thin section studied here includes two clasts of aggregates of euhedral to subhedral enstatite.

Y-791510: This meteorite does not contain chondrules or clasts. The predominant phase is euhedral to subhedral orthoenstatite, 50–200μm in size (Fig. 1f). No plagioclase was encountered. The interstices among enstatite are filled by glassy matrix under the optical microscope. In BSE images, the matrix is divided into homogeneous (Fig. 1g) and devitrified areas (Fig. 1h). The latter is much more abundant ($>$90 vol% of the matrix), and comprises an aggregate of fibrous to fine-grained crystals ($<2\mu$m), with minor amount of unknown dark grains. This meteorite severely experienced terrestrial weathering losing a large amount of opaque minerals. The encountered

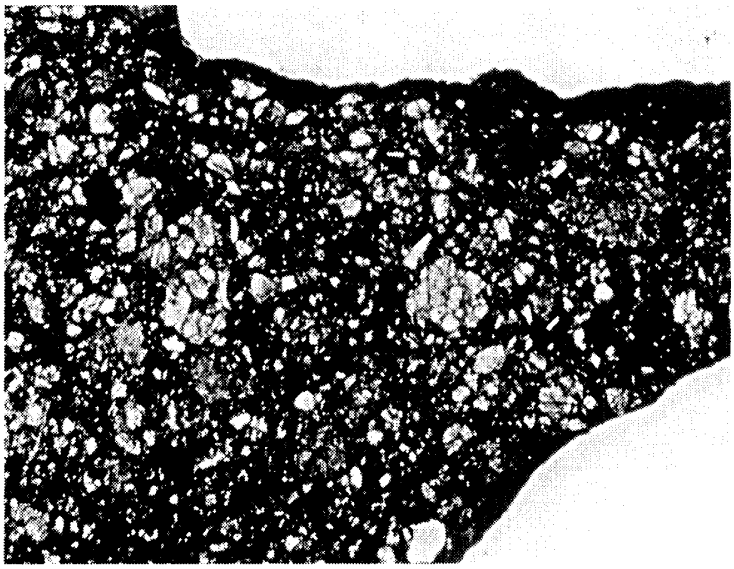

Fig. 1a. Photomicrograph of Y-791810 (EH4). It is noted that chondrules, mostly fragmental, and isolated minerals are abundant. Transmitted light, open nicols, and width of 2.6 mm.

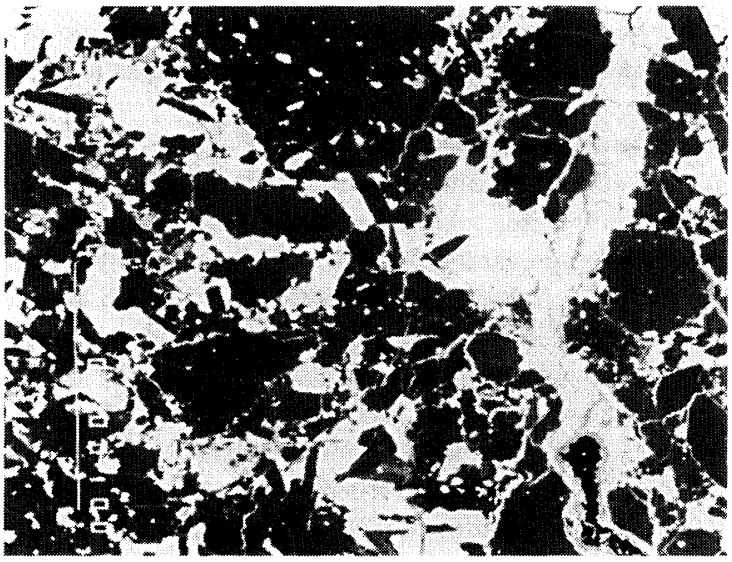

Fig. 1b. Back scatter electron (BSE) image of Y-791810. Although a few euhedral laths of enstatite (dark) occur within opaque minerals (bright), most of enstatite show subhedral to anhedral forms. Width of 0.3 mm.

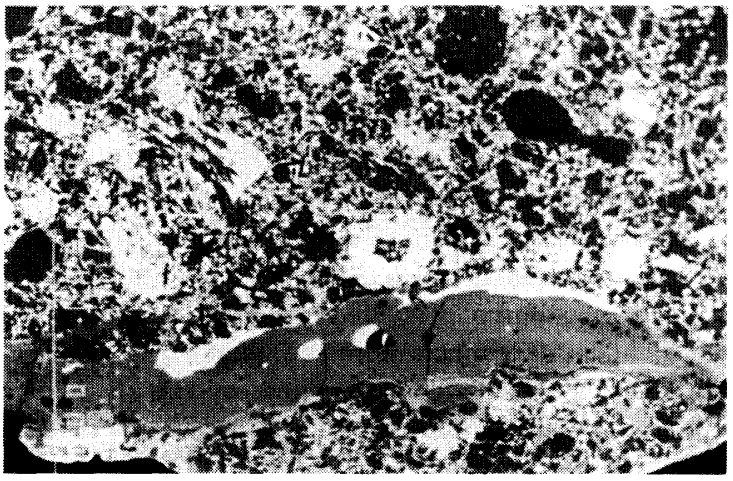

Fig. 1c. BSE image of a melt vein in Y-791790 (EH 4), including opaque mineral aggregates. Width of 2.6 mm.

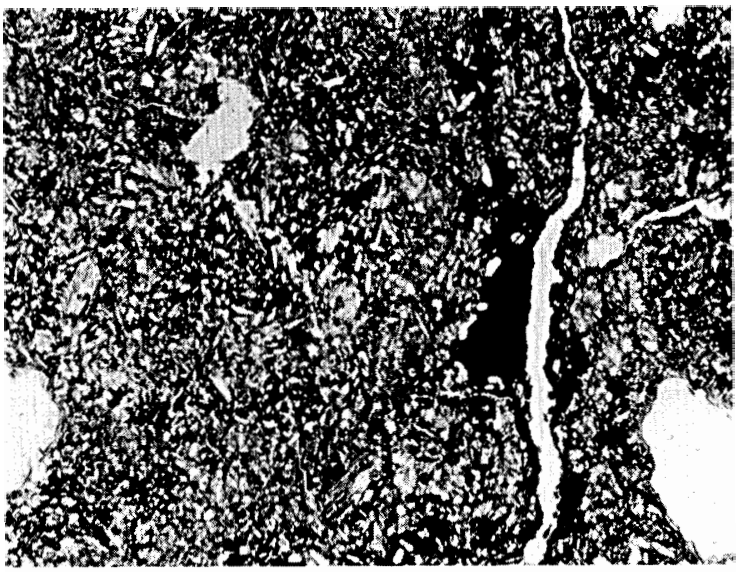

Fig. 1d. Photomicrograph of Y-86760 (EH melt rock) predominantly consisting of euhedral orthoenstatite laths. Chondrule or its fragment is not encountered. Transmitted light, open nicols, and width of 2.6 mm.

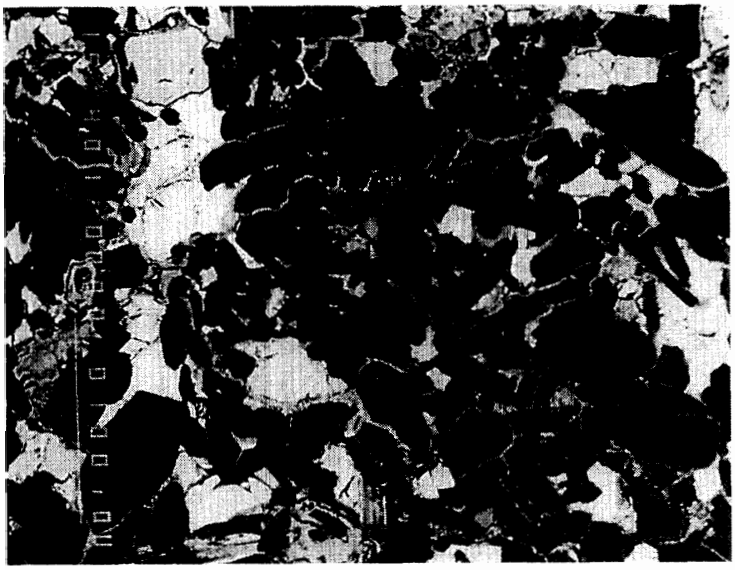

Fig. 1e. BSE image of Y-86760 to show abundant euhedral enstatites. Width of 0.3 mm.

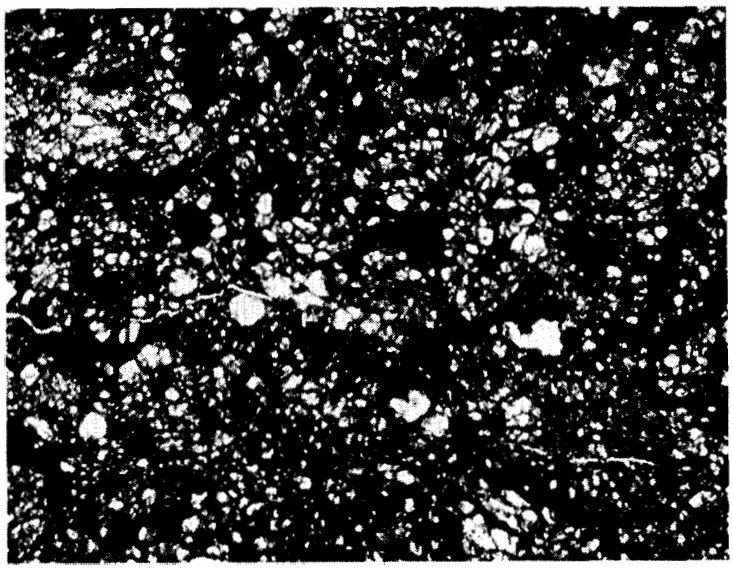

Fig. 1f. Photomicrograph of anomalous Y-791510 containing no chondrule. Transmitted light, open nicols, and width of 2.6 mm.

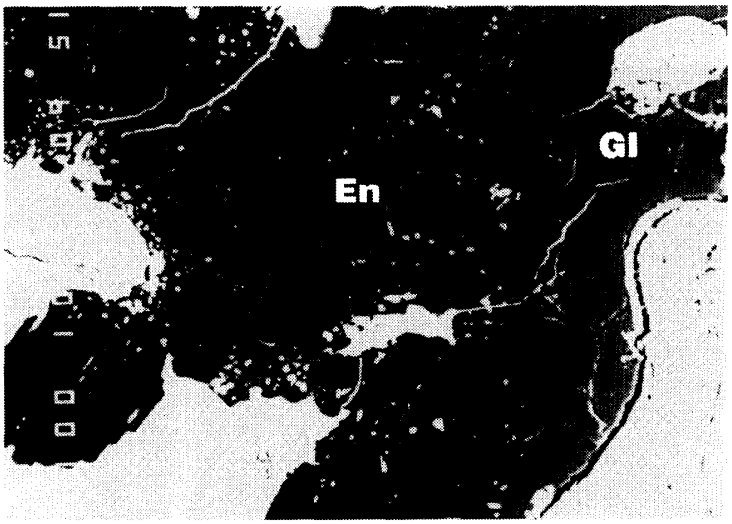

Fig. 1g. Homogeneous glass (Gl) filling the interstices among euhedral to subhedral enstatite (En) in Y-791510. BSE image. Width of 160 μm.

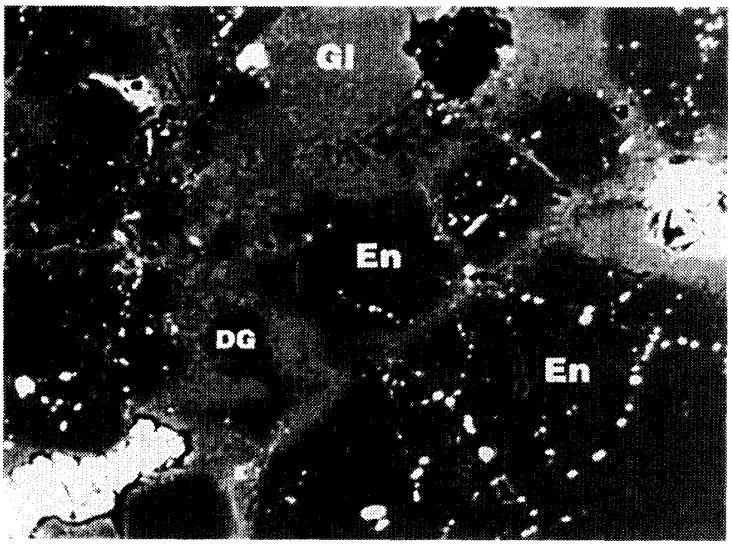

Fig. 1h. Devitrified glass (Gl) in Y-791510, consisting of fibrous to fine-grained crystals with minor amount of dark grains (DG). BSE image. Width of 130 μm.

opaque minerals are kamacite, schreibersite, troilite and daubreelite. Hereafter, we temporarily call Y-791510 an anomalous E-chondrite.

Y-793258: This chondrite is well recrystallized, and contains alabandite, but no niningerite. It is classified as an EL6 chondrite. This is supported by the mineral chemistry (see below).

4. Mineralogy

Forsterite: Forsterite ($Fo_{>99}$) occurs only in the EH3-4 chondrites studied here.

Enstatite: Clinoenstatite occurs in the EH3-4 chondrites, whereas only orthoenstatite in the melt rocks, anomalous E and EL6. Both enstatites are mostly $En_{>98}$ $Wo_{<1}$. As suggested by ZHANG *et al.* (1995), only EH3-4s contain enstatite with >3 wt% FeO (up to Fs_{17}). Enstatite in Y-86760 contains <0.3 wt% Al_2O_3 and <0.4 % CaO (Table 2), similar to those in the other EH melt rocks (LIN and KIMURA, 1998).

Table 2. Representative compositions of silicate phases (wt%).

Phase	Chondrite	Subgroup	SiO_2	TiO_2	Al_2O_3	Cr_2O_3	FeO	MnO	MgO	CaO	Na_2O	K_2O	Total	Fo/En/Ab	Fs/An	Wo/Kf
Forsterite	ALH-77156	EH3	42.01	b.d.	b.d.	0.35	0.78	b.d.	56.00	0.06	b.d.	b.d.	99.27	99.2		
Forsterite	Y-791790	EH4	42.35	b.d.	b.d.	0.19	0.16	0.09	56.86	0.19	b.d.	b.d.	99.89	99.6		
Enstatite	ALH-77156	EH3	54.98	0.06	0.22	0.97	11.40	0.29	30.52	0.46	0.07	b.d.	98.98	81.9	17.2	0.9
Enstatite	ALH-77156	EH3	59.59	0.08	0.40	b.d.	0.19	0.21	38.57	0.65	0.11	b.d.	99.89	98.6	0.3	1.2
Enstatite	Y-791790	EH4	60.06	b.d.	b.d.	b.d.	0.19	b.d.	38.83	b.d.	0.06	b.d.	99.20	99.7	0.3	0.0
Enstatite	Y-791810	EH4	57.46	b.d.	0.83	0.68	7.77	0.17	32.07	1.16	b.d.	b.d.	100.18	86.1	11.7	2.2
Enstatite	Y-791810	EH4	60.04	b.d.	b.d.	b.d.	0.73	b.d.	39.26	b.d.	b.d.	b.d.	100.04	99.0	1.0	0.0
Enstatite	Y-791811	EH4	59.70	b.d.	0.11	b.d.	0.57	b.d.	38.52	0.07	0.32	0.09	99.46	99.1	0.8	0.1
Enstatite	Abee	EH melt	60.49	b.d.	b.d.	b.d.	0.16	b.d.	39.27	0.05	b.d.	b.d.	99.99	99.7	0.2	0.1
Enstatite	Y-86760	EH melt	60.15	b.d.	b.d.	b.d.	0.38	b.d.	39.26	0.24	b.d.	b.d.	100.06	99.0	0.6	0.5
Enstatite	Y-791510	E anom	59.95	b.d.	0.29	0.23	0.27	b.d.	38.43	0.79	b.d.	b.d.	100.00	98.2	0.4	1.4
Enstatite	Y-793258	EL6	60.28	b.d.	0.17	b.d.	b.d.	b.d.	38.77	0.57	b.d.	b.d.	99.86	98.9	0.1	1.0
Plagioclase	ALH-77156	EH3	69.15	0.10	18.58	b.d.	0.29	b.d.	b.d.	b.d.	11.66	0.09	99.91	99.5	0.0	0.5
Plagioclase	Y-791790	EH4	53.55	b.d.	28.90	0.27	0.18	b.d.	0.09	11.99	4.78	0.05	99.81	41.8	57.9	0.3
Plagioclase	Y-791810	EH4	67.71	b.d.	18.75	0.11	0.27	b.d.	b.d.	b.d.	11.55	0.54	98.95	97.0	0.0	3.0
Plagioclase	Y-791811	EH4	68.59	b.d.	18.87	b.d.	0.60	0.13	0.29	0.06	11.33	0.49	100.36	97.0	0.3	2.7
Plagioclase	Y-86760	EH melt	69.20	b.d.	18.38	b.d.	0.43	b.d.	b.d.	b.d.	10.72	1.14	99.99	93.4	0.1	6.5
Plagioclase	Y-793258	EL6	65.63	b.d.	20.34	b.d.	0.31	b.d.	0.11	2.89	9.21	1.14	99.63	79.7	13.8	6.5
Silica mineral	Y-791790	EH4	100.46	b.d.	0.18	b.d.	b.d.	b.d.	0.06	b.d.	0.10	b.d.	100.82			
Silica mineral	Y-86760	EH melt	98.10	b.d.	0.73	0.21	0.32	b.d.	b.d.	b.d.	0.39	0.05	99.91			
Roedderite	ALH-77156	EH3	72.16	b.d.	0.41	b.d.	b.d.	0.11	19.45	b.d.	3.24	4.60	100.01			
Roedderite	Y-791790	EH4	72.81	b.d.	0.29	b.d.	0.43	b.d.	18.54	b.d.	4.46	2.96	99.51			
Roedderite	Y-791810	EH4	73.47	b.d.	0.71	b.d.	0.31	b.d.	19.26	b.d.	4.49	2.99	101.23			
Roedderite	Y-791811	EH4	72.24	b.d.	0.26	b.d.	0.48	b.d.	20.06	b.d.	4.97	2.62	100.65			
Glass homogeneous	ALH-77156	EH3	54.67	b.d.	25.03	0.32	0.25	b.d.	2.54	9.94	6.21	0.07	100.36			
Glass homogeneous	Y-791510	E anom	66.67	b.d.	19.87	0.38	0.11	b.d.	0.95	7.89	4.06	b.d.	99.93			
Glass devitrified	Y-791510	E anom	66.10	b.d.	20.73	0.39	0.76	b.d.	0.08	10.44	1.16	b.d.	99.67			
Glass bulk	Y-791510	E anom	66.77	b.d.	19.81	b.d.	0.58	0.14	1.55	9.00	1.46	b.d.	99.43			
Glass dark grain	Y-791510	E anom	70.10	b.d.	20.52	b.d.	0.32	b.d.	7.82	0.74	0.09	b.d.	99.60			
Vein*	Y-791790	EH4	52.69	b.d.	2.20	0.43	12.74	0.37	26.98	1.83	1.49	0.11	98.87			

*: containing apparent SO_3 (1.44%).

b.d.: below detection limits, 0.03 for Al_2O_3, MgO and CaO, 0.04 for TiO_2, Na_2O and K_2O, 0.08 for FeO and MnO, and 0.10 for Cr_2O_3.

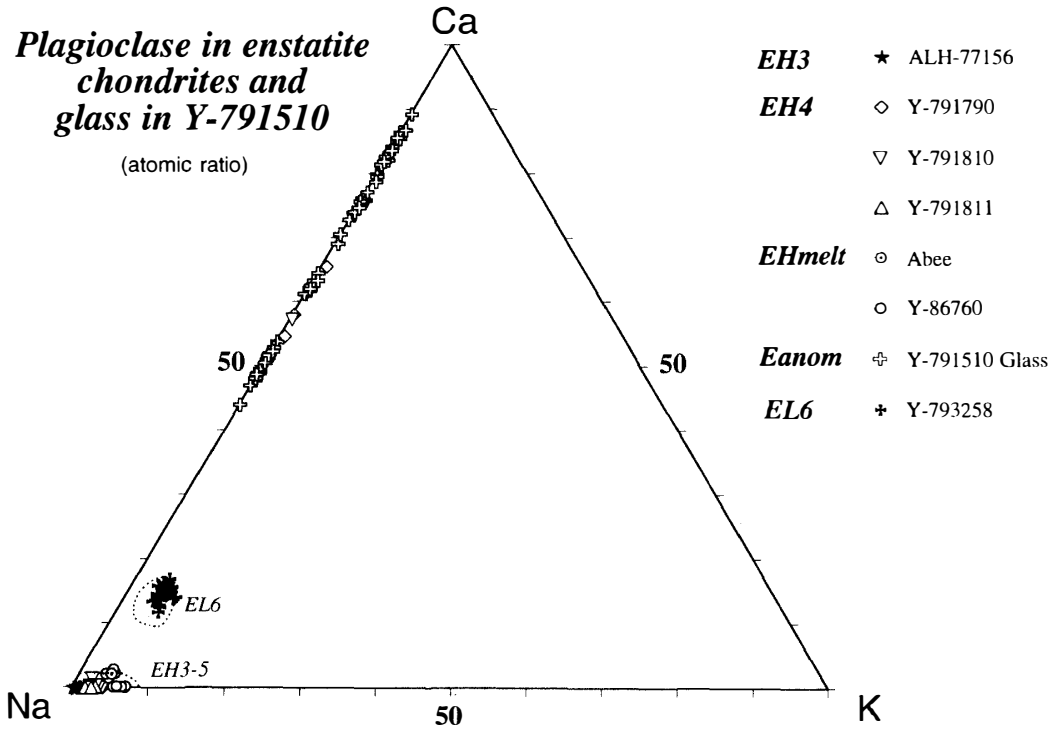

Fig. 2. Ca-Na-K plot of plagioclase and glass in Y-791510. Most of plagioclase are albitic, and only a few grains in the EH3-4s studied here are anorthitic. On the other hand, glass in Y-791510 is unusually enriched in Ca.

Plagioclase: It is mostly albitic in composition (Ab_{96-100} $An_{<1}$ $Or_{<4}$) in the EH3-4s. In contrast, calcic plagioclase (An_{30-65} $Or_{<1}$) often occurs in chondrule groundmasses in the EH3-4s (Fig. 2). Plagioclases in the melt rocks are slightly enriched in K (Ab_{91-95} $An_{<2}$ Or_{4-7}) than those in the EH3-4s. The composition of plagioclase (Ab_{79-83} An_{13-17} Or_{4-7}) in Y-793258 overlaps with those in EL6s (KEIL, 1968).

Silica mineral: It is also a common accessory mineral, and contains 0.1–1.0% Al_2O_3 and 0.1–0.5% Na_2O.

Roedderite: It was only encountered in the EH3-4s. Roedderite (10–70 μm) is usually anhedral to subhedral in shape. As noticed by KIMURA *et al.* (1993), roedderite in EH3 (ALH-77156) is enriched in K_2O (4.6–5.0%) relative to Na_2O (3.0–3.2%) in comparison to those in the EH4s (2.6–3.2% K_2O and 4.3–5.1% Na_2O).

Glassy matrix in Y-791510: It comprises homogeneous and devitrified areas, and the latter is fine-grained aggregate with minor dark grains. Both homogeneous area and fine-grained aggregate are characterized by high concentration of CaO (7.0–8.5 and 7.6–12.9%). They also contain 64.6–67.7 and 57.6–73.6% SiO_2, 19.4–21.5 and 16.5–26.7% Al_2O_3, and 3.9–5.0 and 0.8–2.8% Na_2O, respectively (Table 2). In both areas, the MgO and S contents are lower than 1.0% and below detection limit, 0.1%, respectively. Most of the dark grains contain 68.6–70.1% SiO_2, 19.7–21.3% Al_2O_3 and 7.6–8.8% MgO with <0.7% CaO and <0.2% Na_2O. These phases are not yet identified. The bulk composition of the devitrified area measured using a defocused beam (Table 2) represents 13 wt% normative albite, 46% anorthite, 4% enstatite and 38% silica.

Metallic Fe-Ni: It is usually the most abundant opaque mineral. Metallic Fe-Ni in

Table. 3 Representative compositions of metallic Fe-Ni and schreibersite (wt%).

Phase	Chondrite	Subgroup	Si	P	Fe	Co	Ni	Cu	Total
Metallic Fe-Ni	ALH-77156	EH3	2.59	b.d.	93.47	0.37	2.85	b.d.	99.29
Metallic Fe-Ni	Y-791790 Vein	EH4	0.03	0.74	91.47	0.37	7.21	b.d.	99.98
Metallic Fe-Ni	Y-791790	EH4	3.16	0.31	91.11	0.38	5.48	b.d.	100.48
Metallic Fe-Ni	Y-791810	EH4	3.06	0.34	90.28	0.37	5.60	b.d.	99.66
Metallic Fe-Ni	Y-791811	EH4	3.05	0.11	87.22	0.41	9.38	b.d.	100.20
Metallic Fe-Ni	Abee	EH melt	2.80	0.48	89.13	0.30	7.04	b.d.	99.75
Metallic Fe-Ni	Y-86760	EH melt	2.68	0.18	89.42	0.35	7.46	b.d.	100.09
Metallic Fe-Ni	Y-791510	E anom	3.11	0.20	89.37	0.34	6.78	b.d.	99.84
Metallic Fe-Ni	Y-793258	EL6	1.27	0.11	91.87	0.44	6.03	b.d.	99.75
Perryite	ALH-77156	EH3	12.35	3.34	3.28	b.d.	81.70	0.25	100.96
Schreibersite	Y-791810	EH4	0.27	15.14	77.09	0.32	6.24	b.d.	99.05
Schreibersite	Y-86760	EH melt	0.27	15.15	77.07	0.36	6.40	b.d.	99.32
Schreibersite	Y-791510	E anom	0.22	15.33	66.82	0.10	17.25	b.d.	99.76
Schreibersite	Y-793258	EL6	0.10	15.29	52.63	0.16	30.93	b.d.	99.13

b.d.: below detection limits, 0.02 for Si and P, 0.06 for Co, and 0.09 for Cu.

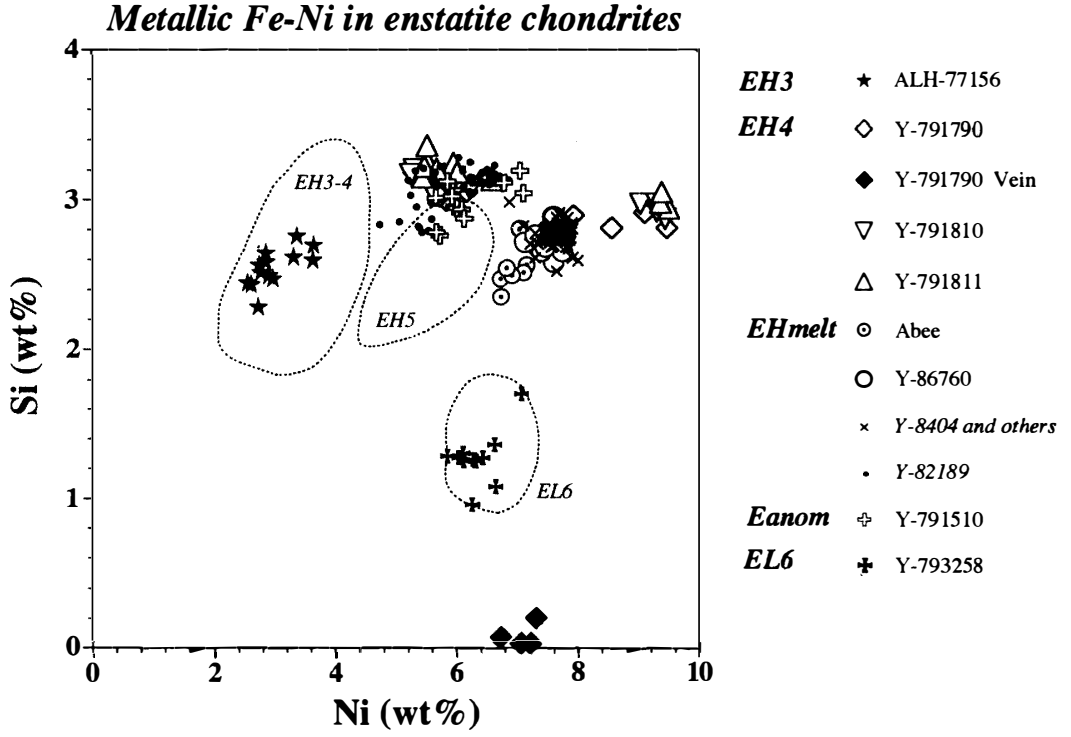

Fig. 3a. Ni vs. Si plot of metallic Fe-Ni. All grains in the EH4s studied here and especially melt rock show higher contents of Ni than those in the other EH3-4s shown by dotted line. Metallic Fe-Ni in vein in Y-791790 is fairly depleted in Si. The compositions in Y-793258 overlap with those of EL6s. The data of Y-8404 and others (Y-8414 and Y-76004), and Y-82189 are after Lin and Kimura *(1998). The compositional ranges of EH3-4s (Y-691, Qingzhen, Y-74370), EH5 (St. Marks) and EL6s are after* Keil *(1968),* El Goresy *et al. (1988),* Kimura *(1988) and* Lin *(1991).*

ALH-77156 contains 2.3–2.8% Si, 2.6–3.6% Ni and <0.05% P (Table 3), thus plotting within the range of EH3-4s (Figs. 3a and b). In comparison, metals in the EH4s studied here contain higher Si (2.8–3.5%), Ni (5.3–9.5%) and P (0.1–0.5%) than those in the other EH3-4s. Metallic Fe-Ni in the melt vein in Y-791790 is enriched in P (0.7–0.9%) and depleted in Si (<0.1%). Those in the melt rocks are enriched in Ni (6.7

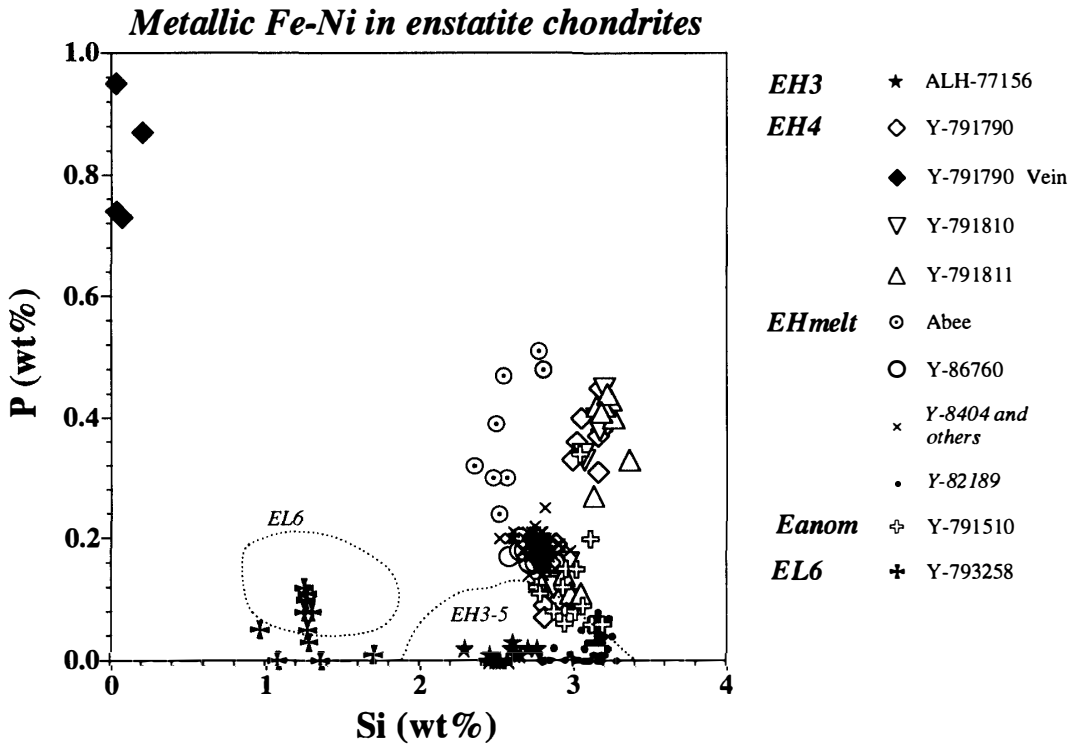

Fig. 3b. Si vs. P plot of metallic Fe-Ni. It is noted that metals in the EH4s studied here, melt rocks and especially vein in Y-791790 have higher contents of P than those in EH3-5s, suggesting high temperature events.

-7.8%) and P (0.16-0.5%) with Si (2.4-2.9%), overlapping with other melt rocks. Compositions of metallic Fe-Ni in Y-793258 (1.0-1.7% Si, 5.8-7.1% Ni, and <0.1% P) overlaps with that in EL6s.

Schreibersite: It abundantly occurs in close association with metallic Fe-Ni. Schreibersites in the EH4s and melt rocks are depleted in Ni (5.7-7.3%). They show overlap with those in Y-8404 and other melt rocks (Fig. 4). Schreibersites in the EH4s are much more depleted in Ni than those in the other EH4s.

Perryite: Only ALH-77156 and Y-793258 contain perryites, in close association with kamacite. Perryite in ALH-77156 contains lower contents of Fe (1.8-4.8%) than that in Y-793258 (5.9-8.3%).

Troilite: Troilite in ALH-77156 contains 0.21-0.32% Ti and 0.3-0.7% Cr (Table 4). In comparison, those in the EH4s are characterized by higher contents of Cr (1.7-2.0%) with 0.23-0.37% Ti (Fig. 5). The grains in Y-791510 are unusually enriched in Ti (0.5-1.3%) with 1.8-2.3% Cr. Troilite in Y-793258 contains 0.6-1.0% Ti and 0.8-1.1% Cr within the range of EL6s.

Daubreelite: It occurs only in ALH-77156, Y-791510 and Y-793258. In Y-791510, daubreelite occurs as fine grain or lamella in troilite, below 10 μm in size. In the other meteorites, it usually occurs as coarse grain, up to 50 μm in size, with troilite. Daubreelites in all three meteorites contain 1.3-2.1% Mn. The content of Zn in ALH-77156 (3.3-4.4%) is higher than those in Y-791510 (below detection) and Y-793258 (<0.1%). No daubreelite was found in the melt rocks and EH4 studied here, although

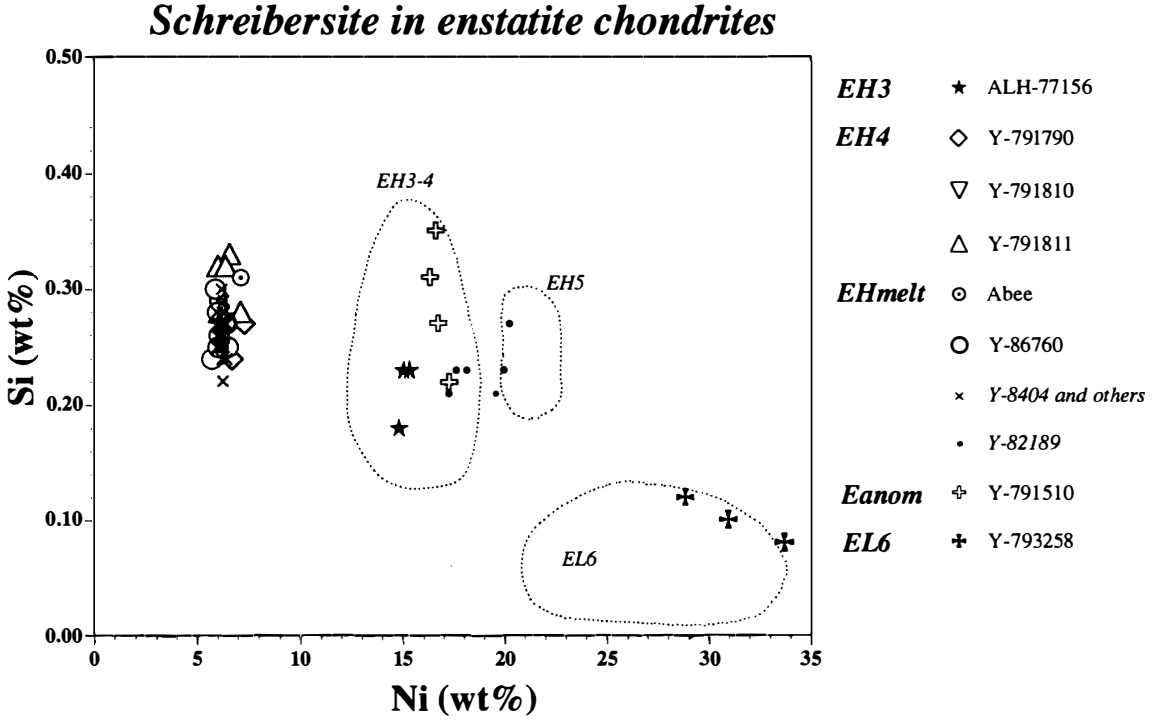

Fig. 4. Ni vs. Si plot of schreibersite. Those in the EH4s and melt rocks studied here are poor in Ni, in comparison with those in EH3-5s.

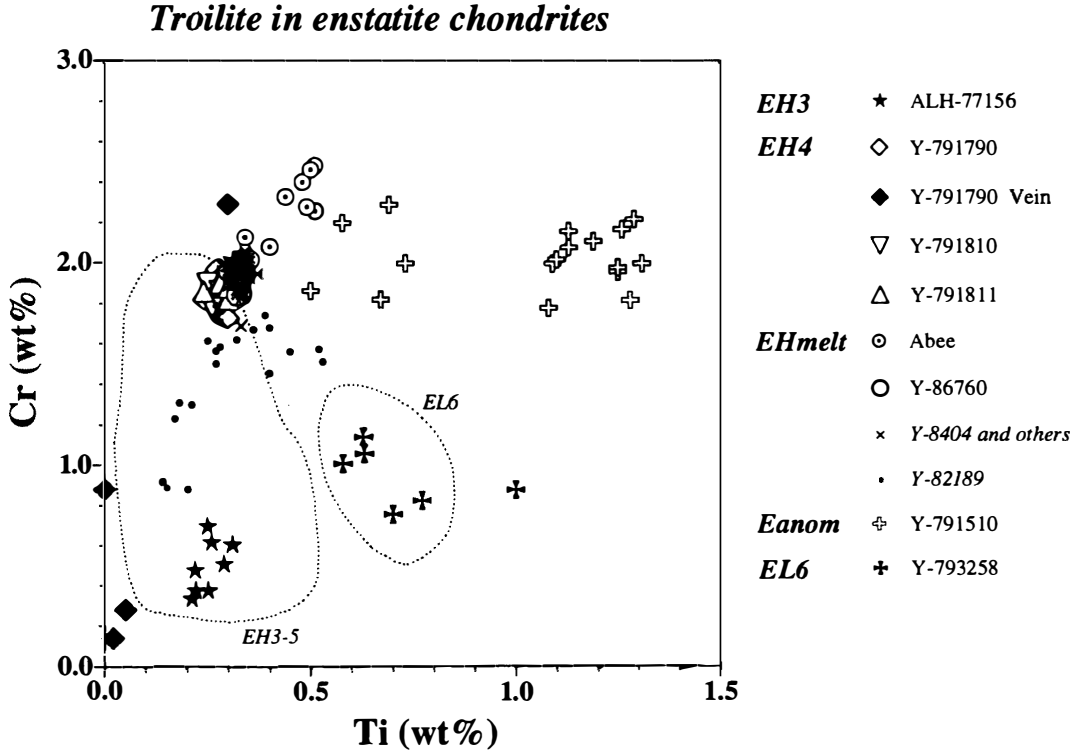

Fig. 5. Ti vs. Cr plot of troilite. The grains in Y-791510 are characteristic of Ti- and Cr-enrichment.

Table 4. Representative compositions of sulfides (wt%).

Phase	Chondrite	Subgroup	Na	Mg	S	Cl	K	Ca	Ti	Cr	Mn	Fe	Ni	Cu	Zn	Ga	Total
Alabandite	Y-793258	EL6	b.d.	3.93	37.65			0.28	b.d.	b.d.	40.79	15.88			0.17		98.74
Daubreelite	ALH-77156	EH3		b.d.	44.08				0.02	34.90	1.46	14.29			3.68		98.43
Daubreelite	Y-791510	E anom		b.d.	42.41				0.09	34.46	1.50	18.13			b.d.		96.60
Daubreelite	Y-793258	EL6		b.d.	43.50				0.05	35.85	1.30	17.42			b.d.		98.11
Djerfisherite	ALH-77156	EH3	0.68		35.39	1.80	9.66			b.d.		46.27	1.22	1.67	b.d.		96.70
Niningerite	Y-791790	EH4	0.84	11.42	42.48			1.79	0.12	1.78	4.78	36.10			b.d.		99.33
Niningerite	Y-791811	EH4	0.86	11.48	41.24			1.82	b.d.	1.93	4.52	35.91			0.17		97.93
Niningerite	Abee	EH melt	1.01	11.04	42.28			2.61	0.06	2.14	3.42	36.66			0.28		99.49
Niningerite	Y-86760	EH melt	0.85	10.76	42.79			1.96	0.08	1.80	3.54	38.05			0.18		100.00
Oldhamite	Abee	EH melt		0.57	39.44			53.50	b.d.	b.d.	0.21	0.54			0.23	0.32	94.82
Sphalerite	ALH-77156	EH3		0.35	35.41			b.d.	b.d.	b.d.	3.30	25.28			32.92	0.51	97.77
Troilite	ALH-77156	EH3		b.d.	36.43				0.31	0.61	b.d.	61.10			0.00		98.50
Troilite	Y-791790 Vein	EH4			34.73				b.d.	0.88	b.d.	61.01	b.d.	0.25			97.15
Troilite	Y-791790	EH4			36.87				0.28	1.83	0.22	59.64	b.d.	b.d.			99.13
Troilite	Y-791810	EH4		b.d.	35.65				0.29	1.85	0.16	60.40			b.d.		98.47
Troilite	Y-791811	EH4		0.05	36.98				0.24	1.86	0.22	59.72			b.d.		99.07
Troilite	Abee	EH melt		b.d.	36.93				0.51	2.48	0.25	59.06			b.d.		99.23
Troilite	Y-86760	EH melt		b.d.	37.13				0.33	1.85	0.14	60.67			b.d.		100.13
Troilite	Y-791510	E anom		b.d.	36.55				1.28	1.82	0.26	59.13			0.17		99.22
Troilite	Y-793258	EL6		b.d.	37.02				0.58	1.01	b.d.	61.07			b.d.		99.84

b.d.: below detection limits, 0.06 for Na and Cl, 0.03 for Mg, K, Ca, Ti and Cr, 0.10 for Mn and Ni, and 0.14 for Cu and Zn.

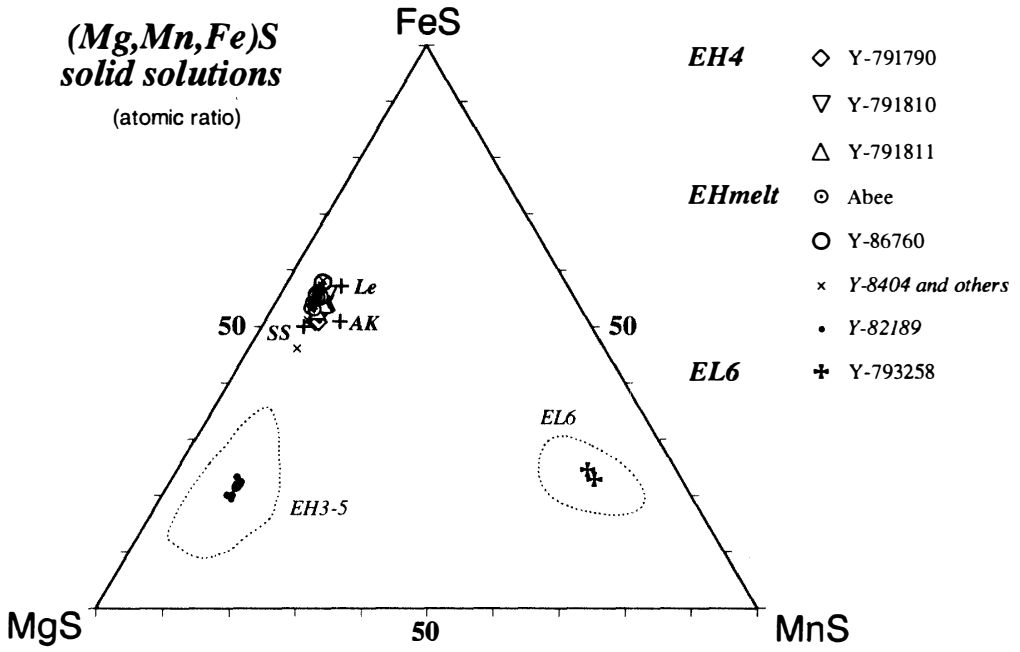

Fig. 6. FeS-MgS-MnS plot of (Mg,Mn,Fe)S solid solutions. Those in the EH4s studied here and melt rocks are FeS-enriched, as well as those in St. Sauveur (SS), LEW88180 (Le) and Adhi Kot (AK). The area denoted by EH3-5 include the data from Y-691, Qingzhen, Y-74370, South Oman, St. Marks, Kaidun III and Indarch. All these data are after KEIL *(1968),* EHLERS *and* EL GORESY *(1988) and* ZHANG *et al. (1995).*

it is common in the other EH4s.

(Mg,Mn,Fe)S: These solid solutions are common in all meteorites, except Y-791510. Niningerites in the EH4s and melt rocks contain 1.5–1.9 and 1.8–2.9% Ca, 10.7–12.8 and 10.2–12.0% Mg, 4.5–5.5 and 3.0–4.2% Mn, and 33.1–36.9 and 34.9–38.1 % Fe, respectively. They show nearly the same compositions as those in the other melt rocks, and have higher Fe (Fig. 6) and Ca contents than those in most EH3-5 chondrites (0.2–1.3% Ca). Y-793258 contains alabandite with 40.0–41.1% Mn and 15.0–16.3% Fe.

Oldhamite: It seems to occur only in Abee, containing 0.6–1.0% Mg, 0.2–0.4% Mn and 0.5–0.9% Fe.

Sphalerite: It is encountered in ALH-77156, Y-791790, Y-791810, Abee and Y-86760, although most of the grains are too small (~5 μm) to be quantitatively analyzed. Sphalerites in the EH4s and melt rock contain higher Mg (0.9–1.3%) and Fe (31.1–33.8 %), but lower Mn (1.3–1.9%) than that in ALH-77156 (0.3–0.4%, 25.1–27.9% and 3.3 –3.7%, respectively).

Djerfisherite: Only ALH-77156 contains djerfisherite, with 1.2–1.7% Ni, 1.1–1.8% Cu, 8.9–9.7% K and 0.5–1.1% Na.

5. Discussion

5.1. *Unusual features of Y-791510*

Y-791510 is evidently an E chondrite, from the occurrences of pure enstatite,

Si-bearing metallic Fe-Ni, Ti- and Cr-bearing troilite and the others. However, the contents of Si in metallic Fe-Ni and schreibersite overlap with those in EHs (Figs. 3 and 4), whereas the low Zn content of daubreelite and high Ti content of troilite are similar to those in EL6.

The occurrences of euhedral enstatite and glassy matrix support that Y-791510 was once melted. A problem is that the matrix is unusually enriched in CaO. Oldhamite might have been decomposed during melting. However, the matrix does not contain S, as mentioned before. The modal abundance of oldhamite in EH chondrites (0.7 vol% after WEISBERG *et al.*, 1995) is too low to account for such CaO-rich matrix. Alternatively, the precursor material may have been primarily enriched in CaO, like some calcic plagioclase-bearing chondrules in the EH3-4 chondrites. From these observations, it is temporarily concluded that Y-791510 belongs to a new grouplet of E chondrites not reported before.

5.2. *Melt vein in Y-791790*

The vein was analyzed by defocused beam (Table 2). After recalculation of the data excluding "FeO" and "SO_3" in assumption that these components represent metal and sulfide, the vein contains 61.1 wt% SiO_2, 2.6% Al_2O_3, 31.3% MgO, 2.1% CaO and 1.7% Na_2O. It is close to the bulk compositions of EH3 chondrites excluding FeO component: 58.3–60.3% SiO_2, 3.0–4.7% Al_2O_3, 31.0–31.5% MgO, 2.0–2.1% CaO and 1.0–1.3% Na_2O after JAROSEWICH (1990) and YANAI and KOJIMA (1995). The modal composition of the vein mentioned before resembles that of EH chondrite (*e.g.*, WEISBERG *et al.*, 1995). Accordingly, the vein was probably derived from melting of EH chondritic material above liquidus temperatures. High P content of the metallic Fe-Ni is consistent with such high temperatures.

FAGAN *et al.* (1998) also found feldspar-dominant veins in an E chondrite, which formed by shock-induced melting and mobilization into the host. It is unusual that metallic Fe-Ni in the vein is Si-free. We speculate that melting took place under more oxidizing conditions than the host.

5.3. *Geothermometries and mineral history*

The diagram of FeS-MgS-MnS system (SKINNER and LUCE, 1971) and FeS contents (~ 50–55 mol%) of niningerites in the EH4s and melt rocks studied here, give closure temperatures of ~800°C, which agree with those of the other melt rocks (LIN and KIMURA, 1998). High FeS contents of sphalerites (~57–58 mol%) in Y-791790 and Y-86760 give ~900°C at p = ~0 kbar, using the FeS-P-T diagram of sphalerite (BALABIN and URUSOV, 1995). Kamacite-schreibersite equilibration temperatures after ZHANG and SEARS (1996) are 730–760°C for the EH4s and 660–790°C for the melt rocks.

All these temperatures are higher than those (~300–600°C) in most of the other EH 3-5 chondrites (ZHANG and SEARS, 1996). This is consistent with the absence of daubreelite in the EH4s and melt rocks studied here, whereas they contain Cr-rich troilites. Daubreelite exsolves from Cr-bearing troilite lower than 600–700°C (EL GORESY and KULLERUD, 1969). The EH4s and melt rocks contain neither perryite nor phases A/B. Although thermal stabilities of these minerals are not yet known, they may be stable at low temperatures. Only a melt rock, Y-82189, contains daubreelite,

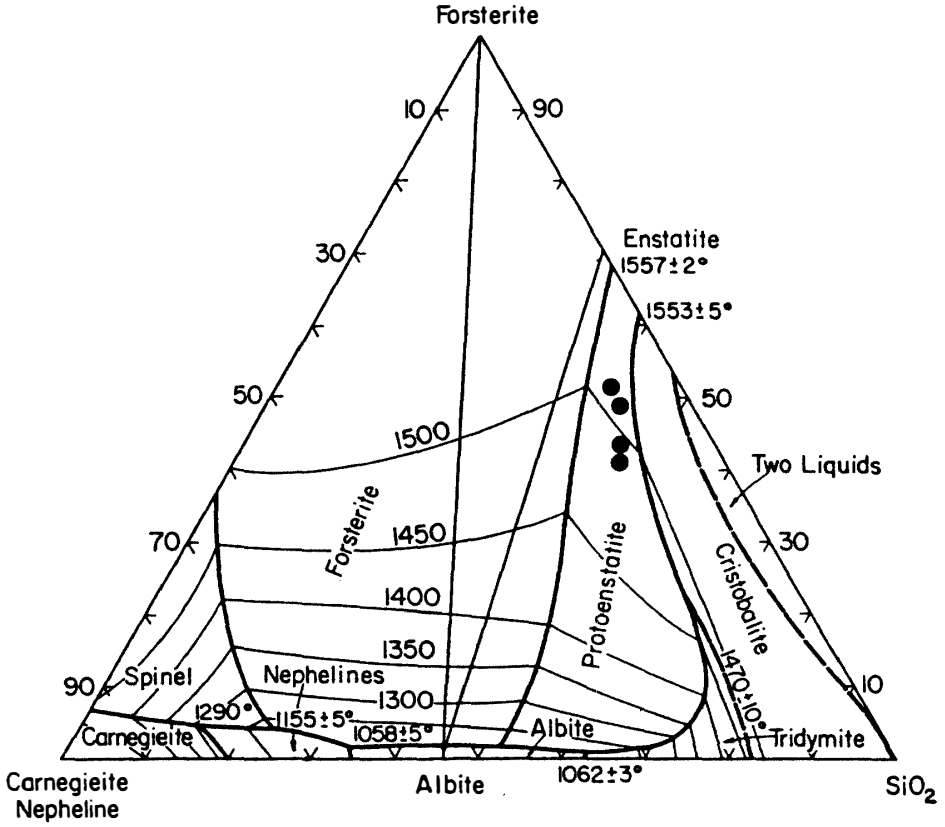

Fig. 7. Plot of modal compositions (filled circles) of the EH melt rocks (Y-86760 in this work; Y-8404 and others after LIN *and* KIMURA, *1998) in the forsterite-nepheline-SiO_2 diagram after* LEVIN *et al. (1964).*

perryite and phases A/B, and this meteorite gives low equilibration temperatures (~400°C) (LIN and KIMURA, 1998).

On the other hand, the absences of roedderite and forsterite are characteristics of all melt rocks. Roedderite is decomposed at 1170°C (ROEDDER, 1951), which is close to the solidus temperature (~1100°C) of silicate portion of EH chondrite (MCCOY *et al.*, 1998). No olivine in the melt rocks is consistent with crystallization from silica-oversaturated EH melts. The modal compositions of the melt rocks are plotted on enstatite liquidus surface in the forsterite-nepheline-silica phase diagram (Fig. 7).

Plagioclases in EH3-4s are almost free from K (atomic Na/Na+K ratios, 0.97–0.99, after KEIL, 1968; KIMURA, 1988; LIN, 1991 and this study), although the bulk ratios are 0.93–0.94 (KALLEMEYN and WASSON, 1986). Djerfisherite (Na/Na+K ratio, 0.11–0.27) and roedderite (0.50–0.70) seem to compensate for K-depleted plagioclases in the EH3-4s. On the other hand, the compositions of plagioclases in the melt rocks (Na/Na+K ratios, 0.94–0.95) are close to the bulk ratio. This suggests that Na and K were completely redistributed into plagioclase during crystallization in the melt rocks.

5.4. Thermal history of EH chondrites

Y-86760, Y-8404, Y-8414 and Y-86004 are melt rocks. Textural features, such as predominant euhedral enstatite grains, and no relic chondrules and grains, suggest that

they were totally melted above liquidus temperatures (~1500°C from forsterite-nepheline-silica diagram and experiment by McCOY *et al.* (1998)). At such temperatures, metallic Fe-Ni and troilite are completely melted. Our studies indicate that enstatite crystallized first from melt. Later, plagioclase, silica mineral, metallic Fe-Ni and troilite crystallized in the interstices among euhedral enstatites. Finally, the meteorites cooled down rapidly from ~800°C. Such a sequence is consistent with crystallization sequence of silica-oversaturated melt, in the forsterite-nepheline-silica phase diagram. In the case of Y-86760, metallic Fe-Ni should have begun to crystallize at about 1200°C from the modal composition and the Fe-FeS phase diagram (KULLERUD, 1967). This can explain the presence of euhedral enstatites enclosed in opaque minerals.

LIN and KIMURA (1998) proposed that these melt rocks were heated by impact near the surface of the parent body, because of melting followed by rapid cooling and very low pressure inferred from sphalerite geobarometer. On the other hand, another melt rock, Y-82189, gives low-equilibration temperatures of the opaque minerals, in spite that the textures of all melt rocks resemble each other. Therefore, these authors proposed that Y-82189 cooled slowly at depth in the parent body, or was reheated at low temperatures.

The studied EH4s give higher temperatures than the other EH4s. However, all these EH4s are similar in texture and mineralogy to each other: devitrification of chondrule mesostasis, sharp boundaries between chondrules and matrices, orthoenstatite with minor clinoenstatite, and the occurrences of forsterite, FeO-bearing enstatite and roedderite. Especially the textural features indicate that the EH4s studied here experienced thermal metamorphism under similar conditions to the other EH4s. The maximum temperature did not exceed the solidus temperature, from the occurrence of roedderite. However, the studied EH4s cooled rapidly from high temperatures (metamorphic stage ?). At any rate, it is noted that EH4s as well as melt rocks show diverse thermal histories, respectively.

One of the characteristic features of E chondrites is high degree of shock metamorphism (RUBIN *et al.*, 1997). In addition, E chondrites abundantly include melt rocks or melt breccias. From the study by RUBIN *et al.* (1997), LIN and KIMURA (1998) and this study, 24 chondrites are types 3 to 5, whereas 5 are melt rocks or melt breccias among EH chondrites, taking pairing into account. In comparison, ordinary chondrites include only about 1% melt rocks (RUBIN, 1995). All these findings suggest that the parent body (or bodies) of EH chondrites was heavily subjected to impact. The melt vein in Y-791790 may be evidence of such impact process. Accordingly, the diverse thermal histories of EH4s and melt rocks could be explained by such an impact process, after or during metamorphism, in the EH parent body. Some EH4s and melt rocks cooled rapidly from high temperatures near the surface of the parent body, whereas the others could be buried in the depth of parent body and cooled slowly, or were later reheated at low temperatures such as ~400°C.

6. Summary

1) Eight E chondrites were studied: 1 EH3, 3 EH4s, 2 EH melt rocks (1 melt breccia), 1 anomalous and 1 EL6.

2) Although the EH4 chondrites studied here show similar textures to the other EH4s, their opaque minerals reflect higher equilibration temperatures than the other EH4s. Such wide variation of mineral history is also noticed in EH melt rocks.

3) The high abundance of melt rocks characterizes EH chondrite group. All these results could be explained by heavy impact on the parent body after or during metamorphism; Some EH4s and melt rocks cooled rapidly from high temperatures near the surface of the parent body, whereas the others cooled slowly in the depth of the parent body, or were later reheated.

4) The anomalous Y-791510 is also a melt rock, but characterized by the occurrence of glassy matrix unusually enriched in CaO. The opaque mineralogy is inconsistent with that of EH or EL. This meteorite belongs to a new grouplet in E chondrites.

Acknowledgments

The sections were supplied by the National Institute of Polar Research (NIPR), Japan. We thank Prof. A. EL GORESY and an anonymous referee for constructive reviews. This work was supported by the Grant-in-Aid for scientific Research from the Ministry of Education, Science and Culture (No. 09640562), Japan Society for Promotion of Sciences (JSPS), and National Natural Science Foundation (NNSF), China, through Grant 49873028.

References

BALABIN, A.I. and URUSOV, V.S. (1995): Recalibration of the sphalerite cosmobarometer: Experimental and theoretical treatment. Geochim. Cosmochim. Acta, **59**, 1401–1410.

EHLERS, E. and EL GORESY, A. (1988): Normal and reverse zoning in niningerite: A novel key parameter to the thermal histories of EH-chondrites. Geochim. Cosmochim. Acta, **52**, 877–887.

EL GORESY, A. and KULLERUD, G. (1969): Phase relations in the system Cr-Fe-S. Meteorite Research, ed. by P.M. MILLMAN. Dordrecht, D. Reidel, 638–656.

EL GORESY, A., YABUKI, H., EHLERS, K., WOOLUM, D. and PERNICKA, E. (1988): Qingzhen and Yamato-691: A tentative alphabet for the EH chondrites. Proc. NIPR Symp. Antarct. Meteorites, **1**, 65–101.

FAGAN, T.J., SCOTT, E.R.D., KEIL, K., COONEY, T.F. and SHARMA, S.K. (1998): Shock melting and mobilization of feldspar-dominated liquid in enstatite chondrite Reckling Peak 80259 (abstract). Meteorit. Planet. Sci., **33**, A46.

JAROSEWICH, E. (1990): Chemical analyses of meteorites: A compilation of stony and iron meteorite analyses. Meteoritics, **25**, 323–337.

KALLEMEYN, G.W. and WASSON, J.T. (1986): Compositions of enstatite (EH3, EH4,5 and EL6) chondrites: Implications regarding their formation. Geochim. Cosmochim. Acta, **50**, 2153–2164.

KEIL, K. (1968): Mineralogical and chemical relationships among enstatite chondrites. J. Geophys. Res., **73**, 6945–6976.

KIMURA, M. (1988): Origin of opaque minerals in an unequilibrated enstatite chondrite, Y-691. Proc. NIPR Symp. Antarct. Meteorites, **1**, 51–64.

KIMURA, M., LIN, Y., IKEDA, Y., EL GORESY, A., YANAI, K. and KOJIMA, H. (1993): Mineralogy of Antarctic aubrites, Yamato-793592 and Allan Hills-78113: Comparison with non-Antarctic aubrites and E-chondrites. Proc. NIPR Symp. Antarct. Meteorites, **6**, 186–203.

KULLERUD, G. (1967): Sulfide studies. Research in Geochemistry, Vol. 2, ed. by P.H. ABELSON. J. Wiley, 286–321.

LEVIN, E.M., ROBBINS, C.R. and MCMURDIE, H.F. (1964): Phase Diagrams for Ceramists. Ohio, The American Ceramic Society, 601p.

LIN, Y. (1991): Qingzhen enstatite chondrite (EH3): Petrology, mineral chemistry and evolution (in Chinese with English abstract). Ph. D. Thesis., The Institute of Geochemistry, Academia Sinica.

LIN, Y. and KIMURA, M. (1998): Petrographic and mineralogical study of new EH melt rocks and a new enstatite chondrite grouplet. Meteorit. Planet. Sci., **33**, 501–511.

MCCOY, T.J., KEIL, K., BOGARD, D.D., GARRISON, D.H., CASANOVA, I., LINDSTROM, M.M., BREARILEY, A. J., KEHM, K., NICHOLS, J.R.H. and HOHENBERG, C.M. (1995): Origin and history of impact-melt rocks of enstatite chondrite parentage. Geochim. Cosmochim. Acta, **59**, 161–175.

MCCOY, T.J., DICKINSON, T.L. and LOFGREN, G.E. (1998): Partial melting of the Indarch (EH4) meteorite: A textural view of melting and melt migration (abstract). Meteorit. Planet. Sci., **33**, A100–A101.

PATZER, A. and SCHULTZ, L. (1998): The exposure age distribution of enstatite chondrites (abstract). Meteorit. Planet. Sci., **33**, A120–A121.

ROEDDER, E.W. (1951): The system K_2O-MgO-SiO_2 Part 1. Am. J. Sci., **249**, 81–130.

RUBIN, A.E. (1995): Petrologic evidence for collisional heating of chondritic asteroids. Icarus, **113**, 156–167.

RUBIN, A.E. and SCOTT, E.R.D. (1997): Abee and related EH chondrite impact-melt breccias. Geochim. Cosmochim. Acta, **61**, 425–435.

RUBIN, A.E., SCOTT, E.R.D. and KEIL, K. (1997): Shock metamorphism of enstatite chondrites. Geochim. Cosmochim. Acta, **61**, 847–858.

SKINNER, B.J. and LUCE, F.D. (1971): Solid solutions of the type (Ca,Mg,Mn,Fe)S and their use as geothermometers for the enstatite chondrites. Am. Mineral., **56**, 1269–1296.

WEISBERG, M.K., BOESENBERG, J.S., KOZHUSHKO, G., PRINZ, M., CLAYTON, R.N. and MAYEDA, T.K. (1995): EH3 and EL3 chondrites: A petrologic-oxygen isotopic study (abstract). Lunar and Planetary Science XXVI. Houston, Lunar Planet. Inst., 1481–1482.

WEISBERG, M.K., PRINZ, M. and NEHRU, C.E. (1997): QUE 94204: An EH-chondrite melt rock (abstract). Lunar and Planetary Science XXVIII. Houston, Lunar Planet. Inst., 1525–1526.

YAMAGUCHI, A., SCOTT, E.R.D. and KEIL, K. (1998): Origin of unusual impact melt rocks, Yamato-790964 and -790143 (LL-chondrites). Antarct. Meteorite Res., **11**, 18–31.

YANAI, K. and KOJIMA, H. (1995): Catalog of the Antarctic Meteorites. Tokyo, Natl Inst. Polar Res., 230p.

ZHANG, Y. and SEARS, D.W.G. (1996): The thermometry of enstatite chondrites: A brief review and update. Meteorit. Planet. Sci., **31**, 647–655.

ZHANG, Y., BENOIT, P.H. and SEARS, D.W.G. (1995): The classification and complex thermal history of the enstatite chondrites. J. Geophys. Res., **100**, 9417–9438.

(Received September 1, 1998; Revised manuscript accepted January 7, 1999)